RevMexAA (Serie de Conferencias), **13**, 222–229 (2002)

NEW RESULTS FROM A SURVEY OF GALACTIC OUTFLOWS IN NEARBY ACTIVE GALACTIC NUCLEI

S. Veilleux,[1] G. Cecil,[2] J. Bland-Hawthorn,[3] and P. L. Shopbell[4]

RESUMEN

Se presentan resultados recientes de un levantamiento multifrecuencia de flujos espacialmente resueltos en galaxias activas cercanas. Se combinan datos espectroscópicos ópticos de Fabry-Perot y de rendija larga con imágenes del VLA (siglas en inglés de "Very Large Array") y de *ROSAT* (siglas en alemán de "*Roentgen Satellit*"), cuando disponibles, para estudiar las componentes gaseosas tibias, relativistas y calientes involucradas en el flujo. Se pone énfasis en objetos que contienen flujos de ángulo amplios y escala galáctica, pero también que muestran evidencia de fenómenos tipo jet colimado a longitudes de ondas de radio y ópticas (p.ej., Circinus, NGC 4388, y con menor intensidad NGC 2992). Nuestros resultados se comparan con las predicciones publicadas de modelos de vientos térmicos impulsados por jets.

ABSTRACT

Recent results from a multiwavelength survey of spatially resolved outflows in nearby active galaxies are presented. Optical Fabry-Perot and long-slit spectroscopic data are combined with VLA and *ROSAT* images, when available, to probe the warm, relativistic and hot gas components involved in the outflow. The emphasis is placed on objects which harbor wide-angle galactic-scale outflows but also show evidence at radio or optical wavelengths for collimated jet-like phenomena (e.g., Circinus, NGC 4388, and to a lesser extent NGC 2992). Our results are compared with the predictions from published jet-driven thermal wind models.

Key Words: **GALAXIES: ACTIVE — GALAXIES: JETS — GALAXIES: KINEMATICS AND DYNAMICS — GALAXIES: SEYFERT — GALAXIES: STARBURST**

1. INTRODUCTION

The main topic at this conference is *jet*-entrained material in Herbig-Haro (HH) objects and in active galactic nuclei (AGN). However, as we discuss in this paper, a significant fraction of AGN harbor poorly collimated winds which may also be of great dynamical significance. A similar wind phenomenon is known to take place in a number of HH objects (e.g., HH 111; Nagar et al. 1997).

A broad range of processes may be responsible for wide-angle outflows in AGN:

1. Starburst-driven winds. The deposition of a large amount of mechanical energy by a nuclear starburst may create a large-scale galactic wind—superwind—which encompasses much of the host galaxy. Depending upon the extent of the halo and its density and upon the wind's mechanical luminosity and duration, the wind may ultimately blow out through the halo and into the intergalactic medium (e.g., Stickland & Stevens 2000 and references therein). The outflow is expected to be wide-angled and oriented roughly along the minor axis of the galactic disk.

2. X-ray heated torus winds. X-rays emitted in the inner part of an accretion disk can Compton-heat the surface of the disk further out, producing a corona and possibly driving off a wind (e.g., Begelman, McKee, & Shields 1983; Krolik & Begelman 1986, 1988; Balsara & Krolik 1993). For Seyfert galaxies, a substantial wind with $T_{\rm wind} \approx 1 \times 10^6$ K and $V_{\rm wind} \approx 200$–500 km s^{-1} is driven off if $L/L_{\rm E} \gtrsim 0.08$ (e.g., Balsara & Krolik 1993). The wind is directed along the minor axis of the *accretion* disk and is not necessarily perpendicular to the *galactic* disk.

3. Jet-driven thermal winds. AGN-driven jets entrain and heat gas on kiloparsec scales. The internal energy densities of these loosely collimated jets may be dominated by thermal X-ray-emitting plasma. The extended soft X-ray emission from these objects should be roughly cospatial with the large-scale radio emission, as seen in some active galaxies (e.g., Colbert et al. 1996, 1998). The transport of energy and momentum by these "mass-loaded" jets may be able to power the narrow-line regions of Seyferts (e.g., Bicknell et al. 1998).

[1]Dept. of Astronomy, U. Maryland, USA.
[2]Dept. of Physics and Astronomy, U. North Carolina, USA.
[3]Anglo-Australian Observatory, Australia.
[4]Dept. of Astronomy, California Inst. of Technology, USA.

In the rest of this paper, we aim to determine which one(s) of these mechanisms is (are) responsible for the wide-angle outflows seen in AGN. In § 2, we describe a survey our group has been conducting over the years on nearby AGN. In § 3, we summarize the general trends that we see in our data and address the issues of the ionization source of the line-emitting material and the energy source of the outflows. In § 4, we discuss the recent results on three objects representative of our sample: Circinus, NGC 2992, and NGC 4388. We summarize our conclusions and discuss future avenues of research in § 5.

2. DESCRIPTION OF SURVEY

Over the past ten years, our group has been conducting an optical survey of nearby active and starburst galaxies combining Fabry-Perot imaging and long-slit spectrophotometry with radio and X-ray data to track the energy flow of galactic winds through the various gas phases. The complete spatial and kinematic sampling of the Fabry-Perot data is ideally suited to study the complex and extended morphology of the warm line-emitting material which is associated with the wind flow. The radio and X-ray data complement the Fabry-Perot data by probing the relativistic and hot gas components, respectively.

Our sample contains twenty active galaxies with known galactic-scale outflows. Half of them are Seyfert galaxies and the rest are starburst galaxies (not discussed here; the outflows in these objects are starburst-driven winds). All of these objects are nearby ($z < 0.01$ to provide a spatial scale of < 200 pc arcsec^{-1}) and have line-emitting regions that extends more than $30''$. So far, the results have been published for about a dozen of these objects. Table 1 lists the main papers which have come out from our survey.

TABLE 1

SOME KEY PUBLICATIONS

Galaxy	Reference
M 51	Cecil (1988)
M 82	Bland & Tully (1988)
	Shopbell & Bland-Hawthorn (1998)
NGC 1068	Cecil et al. (1990)
	Bland-Hawthorn et al. (1991)
	Sokolowski et al. (1991)
	Cecil et al. (2002)
NGC 2992	Veilleux et al. (2001)
NGC 3079	Veilleux et al. (1994)
	Veilleux et al. (1995)
	Veilleux et al. (1999a)
	Cecil et al. (2001)
NGC 3516	Veilleux et al. (1993)
NGC 4258	Cecil et al. (1992)
	Cecil et al. (1995)
	Cecil et al. (1995)
	Cecil et al. (2000)
NGC 4388	Veilleux et al. (1999a)
	Veilleux et al. (1999b)
NGC 6240	Bland-Hawthorn et al. (1991)
Circinus	Veilleux & Bland-Hawthorn (1997)

3. GENERAL RESULTS

Evidence for loosely collimated winds are detected in several AGN. Approximately 75% of the AGN in our (admittedly biased) sample harbor wide-angle outflows rather than collimated jets. These outflows typically show the following optical properties:

- The optical winds are often lopsided and sometimes tilted with respect to the polar axis of the host galaxy (e.g., NGC 4388).
- The solid angle subtended by these winds, $\Omega_{\rm W}/4\pi \approx 0.1$–$0.5$.
- The radial extent of the line-emitting material involved in the outflow, $R_{\rm W} = 1$–5 kpc.
- The outflow velocity of the line-emitting material, $V_{\rm W} = 100$–1500 km s^{-1} regardless of the escape velocity of the host galaxy. Until recently the record holder was NGC 3079, where outflow velocities in excess of 1500 km s^{-1} are directly measured (Veilleux et al. 1994). But the outflow velocities in NGC 1068 are now known to be far larger than this value (see Cecil, Ferruit, & Veilleux 2002, these proceedings, and Cecil et al. 2002).
- The dynamical time scale, $t_{\rm dyn} \approx R_{\rm W}/V_{\rm W} = 10^6$–$10^7$ years.
- The ionized mass involved in the outflow, $M = 10^5$–10^7 $M_\odot$, a relatively small fraction of the total ISM in the host galaxy.
- The ionized mass outflow rate, $dM/dt \approx M/t_{\rm dyn} = 0.1$–$1$ $M_\odot$ yr^{-1} $> dM_{\rm acc}/dt$, the mass accretion rate necessary to fuel the AGN.
- The kinetic energy of the outflowing ionized material, $E_{\rm kin} = 10^{53}$–10^{55} erg, taking into account both the bulk and "turbulent" (spectrally unresolved) motions. This mechanical energy is equivalent to that of $\sim 10^2$–10^4 Type II SNe.
- The kinetic energy rate of the outflowing ion-

Emission Lines from Jet Flows (Isla Mujeres, Q.R., México, November 13-17, 2000)
Editors: W. J. Henney, W. Steffen, A. C. Raga, & L. Binette

ized material, $dE_{\rm kin}/dt \approx E_{\rm kin}/t_{\rm dyn}$ = few $\times$ 10^{39}–10^{42} erg s^{-1}.

• Evidence for entrainment of (rotating) disk material is seen in some objects (e.g., Circinus, NGC 2992, NGC 3079).

• The source of ionization of the line-emitting material taking part in these outflows is diverse. Pure photoionization by the AGN can explain the emission-line ratios in NGC 3516 and NGC 4388. Shock ionization is probably contributing in Circinus and NGC 2992.

• Starburst-driven winds are not common among AGN (a possible exception is NGC 3079; Veilleux et al. 1994; Cecil et al. 2001). Galactic winds are roughly aligned with galaxy-scale (several kpc) radio emission, sometimes encompassing what appears to be poorly collimated radio "jets". These mass-loaded "jets" are the probable driving engine for these winds. In most cases, however, torus-driven winds cannot formally be ruled out.

4. CASE STUDIES OF THREE NEARBY AGN

In this section, we discuss the recent results on Circinus, NGC 2992, and NGC 4388, three fairly representative objects of our sample. While the morphology and kinematics of the optical outflows in these objects are very different, they appear fundamentally to be driven by the same process, namely entrainment along poorly collimated "jets". For more information on these objects, the reader should refer to the original papers: Veilleux & Bland-Hawthorn (1997), Veilleux et al. (2001), and Veilleux et al. (1999a,b), respectively.

4.1. *Circinus*

The Circinus galaxy is the nearest ($\sim$ 4 Mpc) Seyfert 2 galaxy known, and is therefore ideally suited for detailed studies of AGN-driven outflows. Recent maps (Elmouttie et al. 1995, 1998) have resolved spectacular radio lobes centered on the nucleus, and extending more than 90$''$ ($\sim$ 2 kpc) on either side of the galaxy disk (PA $\approx -60°$).

4.2. *Morphology and Kinematics of the Line-Emitting Material*

Our Fabry-Perot data on Circinus (Figure 1) reveal a complex of ionized filaments extending radially from the nucleus out to distances of 1 kpc. The most striking [O III] feature extends along position angle $\sim -50°$ spanning a distance of $\sim$ 25–45$''$ (500–900 pc) from the nucleus. The lateral extent of this filament is near the limit of our resolution ($\sim$ 1$''$.5 after smoothing). This narrow feature is also visible

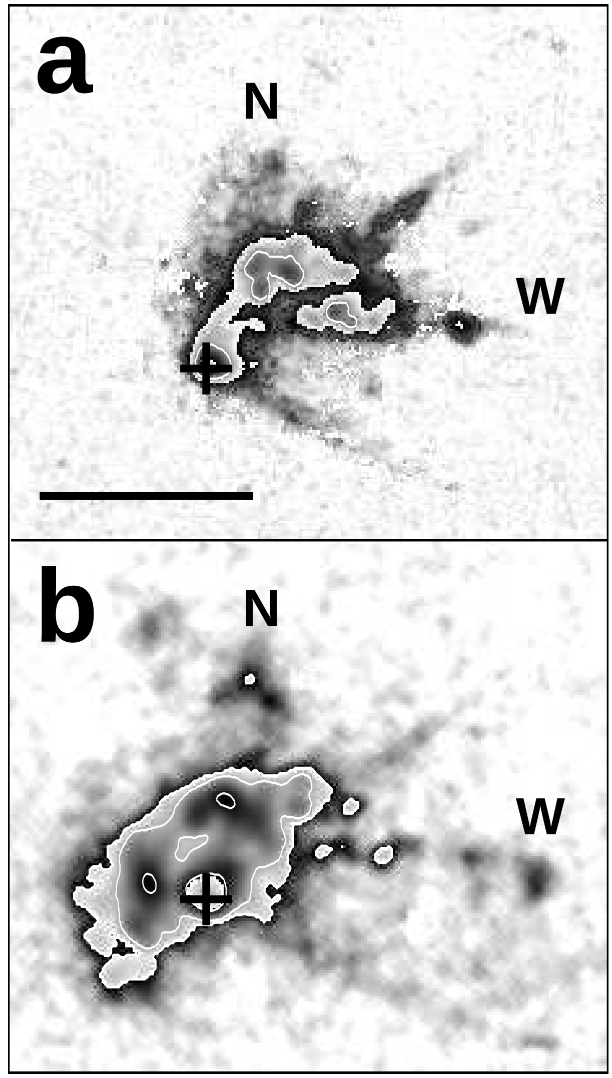

Fig. 1. Line flux images of the Circinus galaxy: (a) [O III] λ 5007 and (b) blueshifted (between -150 and 0 km s^{-1}) Hα. North is at the top and west to the right. The position of the infrared nucleus (Marconi et al. 1995) is indicated in each image by a cross. The spatial scale, indicated by a horizontal bar at the bottom of the [O III] image, is the same for each image and corresponds to $\sim$ 25$''$ or 500 pc for the adopted distance of the Circinus galaxy of 4 Mpc. The minor axis of the galaxy runs along PA $\approx -60°$.

in Hα but with a lower contrast. The gas at this location is highly ionized with a [O III] λ 5007/Hα flux ratio typically larger than unity. Extrapolation of this filament to smaller radii comes to within 1$''$ (20 pc) of the infrared nucleus (Marconi et al. 1995), suggesting a nuclear (most likely AGN) origin to this feature.

The most spectacular feature in the Hα data is the hook-shaped filament which extends to 40$''$

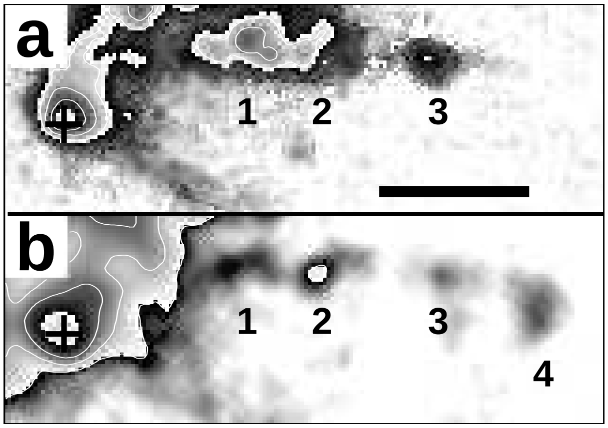

Fig. 2. Line flux images of the western hook-shaped filament: (a) [O III] $\lambda\,5007$ and (b) blueshifted (between -150 and 0 km s^{-1}) Hα. The position of the infrared nucleus (Marconi et al. 1995) is indicated in each image by a cross. The orientation is the same as in Fig. 1, but the horizontal bar at the bottom of the [O III] image now corresponds to ~ 250 pc.

(800 pc) west of the nucleus (Figure 2). Such features are commonly observed in HH objects although they have never been seen on galactic scales. Additional morphological evidence for outflow exists in the northern portion of our data. The [O III] emission along PA $\approx -20°$ forms a broad filamentary 'finger' or jet that points back to the nucleus. A knot is present at the tip of this 'finger', $25''$ from the nucleus. Bright Hα emission is also visible near this position, the southern portion of which forms a wide ($\sim 8''$) arc resembling a bow shock. The arc is pointing in the downstream direction consistent with being produced by a collimated jet.

The kinematics derived from the [O III] Fabry-Perot data and complementary long-slit spectra bring credence to the nuclear outflow scenario. Non-gravitational motions are observed throughout the [O III] cone, superposed on a large-scale velocity gradient caused by galactic rotation along the major axis of the galaxy (PA$_{\rm maj}$ $\approx 30°$; Freeman et al. 1977). Sudden velocity gradients are seen near the positions of the bright [O III] and Hα knots.

4.2.1. *Source of Ionization*

The motions observed across the ionization cone are highly supersonic, so high-velocity ($V_{\rm s} \gtrsim 100$ km s^{-1}) shocks are likely to contribute to the ionization of the line emitting gas. Large variations of the line ratios are sometimes observed within a single knot (Figure 3). The enhanced [N II]/Hα, [S II]/Hα, and [O III]/Hβ ratios in knots 1 and 2 fall near the range produced by the high velocity photoionizing radiative shocks of Dopita & Sutherland (1995). Photoionization purely by the active nucleus of a mixture of ionization and matter-bounded clouds whose relative proportions vary with position in the galaxy may also provide another explanation for the abrupt changes of excitation in the filaments (e.g., Binette, Wilson, & Storchi-Bergmann 1996).

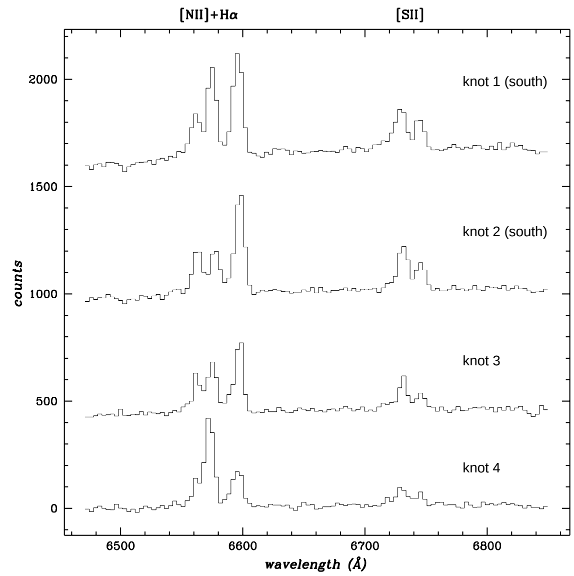

Fig. 3. Binned spectra at four positions along the slit through the nucleus corresponding to knots 1–4 in Fig. 2. Each spectrum has been offset by 400 counts. Knots 1 and 2 are binned along the slit over $6''$; knots 3 and 4 are binned over $4''$. Note the greatly enhanced [N II]/Hα ratio along the jet, except on the bow shock at knot 4.

4.2.2. *Nature of the Outflow*

The mass of ionized gas involved in this outflow is fairly modest, $\sim$ few $\times 10^4 X^{-1} n_{\rm e,2}^{-1}\, M_\odot$ where X is the fraction (< 1) of oxygen which is doubly ionized and $n_{\rm e,2}$ is the electron density in units of 100 cm^{-3}. The total kinetic energy ($\sim 10^{53} n_{\rm e,2}^{-1}$ erg) lies near the low energy end of the distribution for wide-angle events observed in nearby galaxies. The morphology and velocity field of the filaments suggest that they represent material expelled from the nucleus (possibly in the form of "bullets") or entrained in a wide-angle wind roughly aligned with the radio "jet" and the polar axis of the galaxy. The complex morphology of the outflow in the Circinus galaxy is unique among active galaxies. The event in the Circinus galaxy may represent a relatively common evolutionary phase in the lives of gas-rich active galaxies during which the dusty cocoon surrounding the nucleus is expelled by the action of jet or wind phenomena.

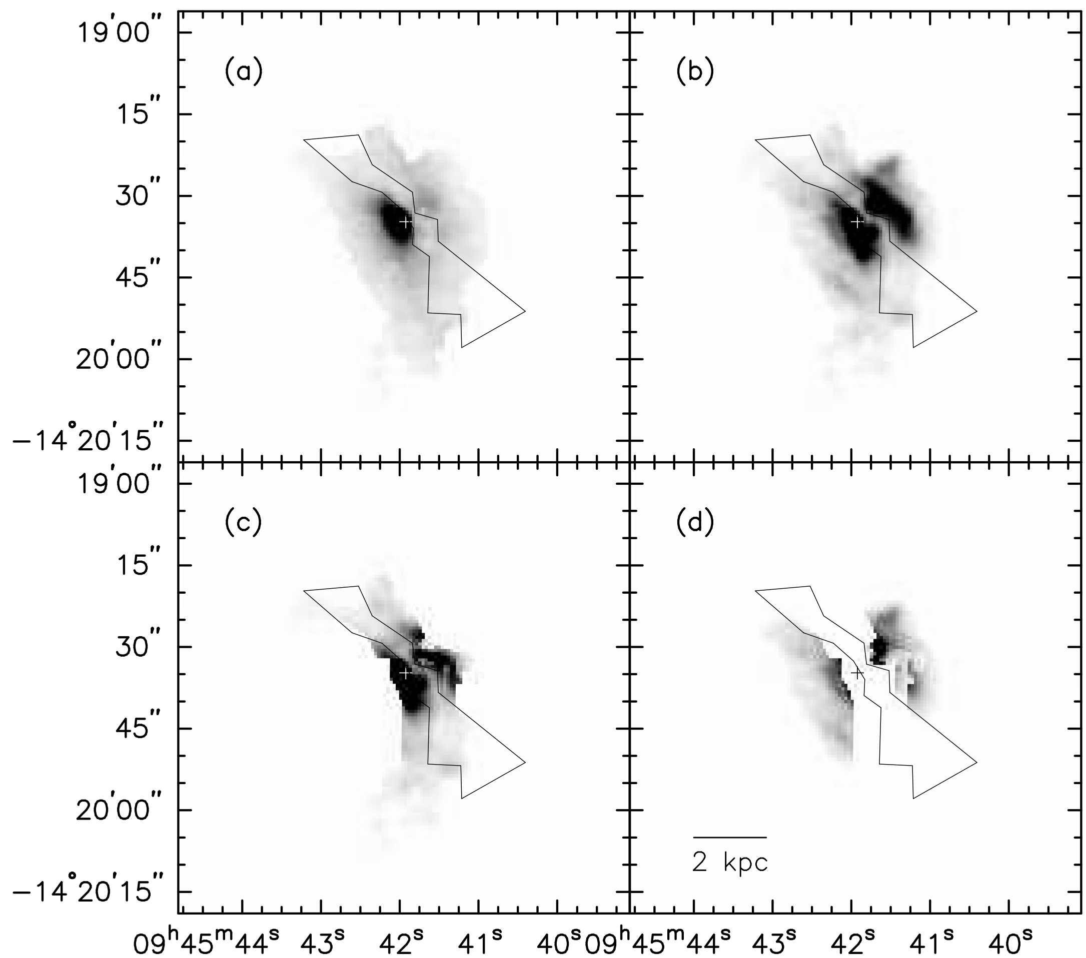

Fig. 4. Distribution of the Hα and continuum emission in NGC 2992. (a) Continuum emission at rest wavelength $H\alpha$, (b) total Hα emission, (c) Hα emission from the disk component, (d) Hα emission from the outflow component. The position of the radio nucleus ("+") and the extent of the dust lane are indicated on each of these panels. North is at the top and east to the left. Note the absence of a disk component in the east quadrant.

Emission Lines from Jet Flows (Isla Mujeres, Q.R., México, November 13-17, 2000)
Editors: W. J. Henney, W. Steffen, A. C. Raga, & L. Binette

4.3. *NGC 2992*

The presence of a galactic-scale outflow in NGC 2992 has been suspected for several years, based on the morphology of the radio emission (Ward et al. 1980; Hummel, van Gorkom, & Kotanyi 1983) and more recently the X-ray emission (Colbert et al. 1998). In the optical, the line emission from the outflow is severely blended with line emission from the galactic disk. The complete two-dimensional coverage of our Fabry-Perot data is therefore critical to disentangle the material associated with the wind from the gas in rotation in the galactic disk.

4.3.1. *Morphology and Kinematics of the Outflowing Line-Emitting Material*

The distribution of the Hα-emitting gas in the disk and outflow components is shown in Figure 4. The outflow component (Fig. 4d) is distributed into two wide cones which extend up to $\sim 18''$ (2.8 kpc) from the peak in the optical continuum map. Both cones have similar opening angles of order 125–135°. The bisectors of each of the cones coincide with each other and lie along PA $\approx$ 116°, or almost exactly perpendicular to the kinematic major axis of the inner disk (PA $\approx$ 32°). This strongly suggests that the axis of the bicone is perpendicular to the galactic disk, and that the material in the SE cone is emerging from under the galaxy disk while the material in the NW cone is emerging from above the disk.

The outflow on the SE side of the nucleus is made of two distinct kinematic components interpreted as the front and back walls of a cone. The azimuthal velocity gradient in the back-wall component reflects residual rotational motion which indicates either that the outflowing material was lifted from the disk or that the underlying galactic disk

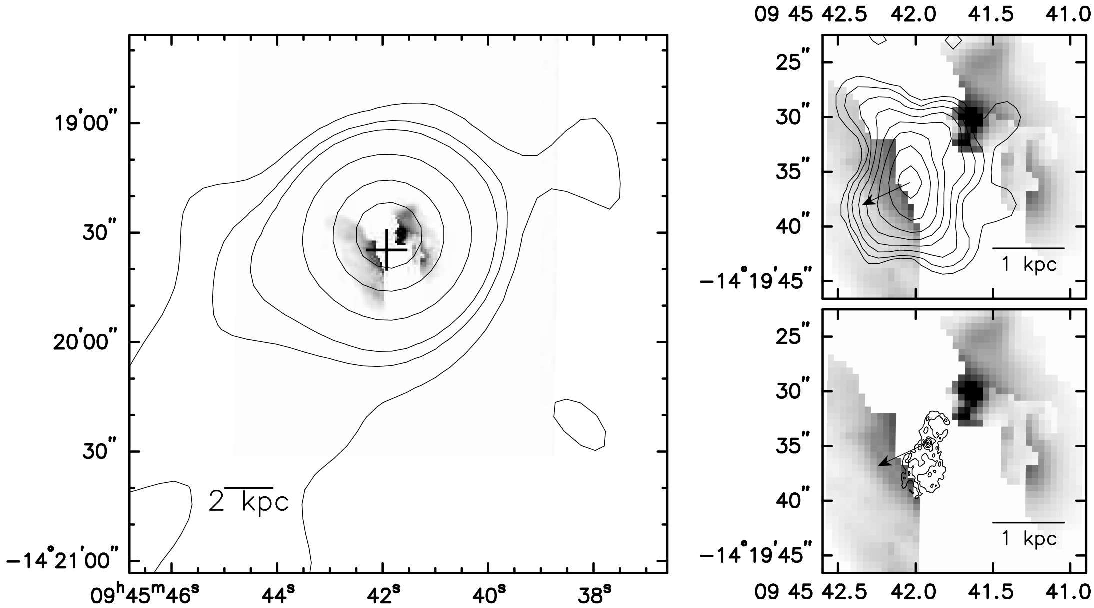

Fig. 5. Contour maps of the X-ray emission (left panel: *ROSAT*/HRI data from Colbert et al. 1998) and 6-cm continuum emission (upper right panel: VLA C-configuration data from Colbert et al. 1996 with 3″ uniform weighting; lower right panel: VLA A-configuration data from Ulvestad & Wilson 1984) superimposed on the total Hα emission from NGC 2992 (grey-scale). A cross ("+") in the main figure indicates the position of the radio nucleus. The arrows in the right panels mark the direction of the one-sided 90″ (13.5 kpc) radio extension along P.A. $\sim$ 100–130°, i.e., close to the axis of the biconical outflow. Same orientation as Fig. 4.

is contributing slightly to this component. A single outflow component is detected in the NW cone.

4.3.2. *Source of the Outflow*

A biconical outflow model with velocities ranging from 50 to 200 km s^{-1} and oriented nearly perpendicular to the galactic disk can explain most of the data. The broad line profiles and asymmetries in the velocity fields suggest that some of the entrained line-emitting material may lie inside the biconical structure rather than only on the surface of the bicone. The mass involved in this outflow is of order $\sim 1 \times 10^7 n_{\rm e,2}^{-1}\ M_\odot$, and the bulk and "turbulent" kinematic energies are $\sim 6 \times 10^{53} n_{\rm e,2}^{-1}$ erg and $\sim 3 \times 10^{54} n_{\rm e,2}^{-1}$ erg, respectively. The faint X-ray extension detected by Colbert et al. (1998) and shown in Figure 5 lies close to the axis of the outflow bicone, suggesting a possible link between the hot and warm gas phases in the outflow. The position angles of the optical outflow bisector and the long axis of the "figure-8" radio structure shown in Figure 5 differ by $\sim$ 25–35°, but the one-sided 13.5-kpc radio extension detected by Ward et al. (1980) and Hummel et al. (1983) lies roughly along the same direction as the mid-axis of the SE optical cone (PA $\sim$ 100–130°; arrows mark this direction in the right panels of Fig. 5). The most likely energy source of the optical outflow is a hot bipolar thermal wind powered on sub-kpc scale by the AGN and diverted along the galaxy minor axis by the pressure gradient of the ISM in the host galaxy. The data are not consistent with a starburst-driven wind or a collimated outflow powered by radio jets.

4.4. *NGC 4388*

NGC 4388 was the first Seyfert galaxy discovered in the Virgo cluster (Phillips & Malin 1982). It is plunging edge-on at 1500 km s^{-1} through the center of the Virgo cluster and experiencing the effects of ram-pressure stripping by the densest portions of the intracluster medium (ICM; e.g., Cayatte et al. 1994). Nuclear activity has been detected at nearly all wavelengths. The morphology of the nuclear radio source suggests a collimated AGN-driven outflow (Stone, Wilson, & Ward 1988; Falcke, Wilson, & Simpson 1998). At optical wavelengths, NGC 4388 has been known for some time to present extended line emission (e.g., Pogge 1988; Corbin, Baldwin, & Wilson 1988 and references therein). A rich complex of ionized gas extends both along the disk of the galaxy and up to 50″ (4 kpc) above that plane. The extraplanar gas component has considerably higher

Emission Lines from Jet Flows (Isla Mujeres, Q.R., México, November 13-17, 2000)
Editors: W. J. Henney, W. Steffen, A. C. Raga, & L. Binette

ionization than the disk gas, and appears roughly distributed into two opposed radiation cones that emanate from the nucleus (Pogge 1988; Falcke et al. 1998). Detailed spectroscopic studies strongly suggest that this component is mainly ionized by photons from the nuclear continuum (Pogge 1988; Colina 1992; Petitjean & Duret 1993).

4.4.1. *Morphology and Kinematics of the Extraplanar Line-Emitting Material*

Figure 6 shows the distribution of the line-emitting material in this galaxy derived from our Fabry-Perot data. We confirm the existence of a rich complex of highly ionized gas that extends $\sim$ 4 kpc above the disk of this galaxy. Low-ionization gas associated with star formation is also present in the disk. Evidence for bar streaming is detected in the disk component and is discussed in Veilleux et al. (1999a,b). Non-rotational blueshifted velocities of 50–250 km s^{-1} are measured in the extraplanar gas north-east of the nucleus. The brighter features in this complex tend to have more blueshifted velocities. A redshifted cloud is also detected 2 kpc south-west of the nucleus. The total mass and kinetic energy of the extraplanar gas are $\sim 4\times10^5$ $M_\odot$ and $E_{\rm kin} = E_{\rm bulk}+E_{\rm turb} \gtrsim 1\times10^{53}$ erg, respectively.

4.4.2. *Geometry of the Outflow*

The velocity field of the extraplanar gas of NGC 4388 appears to be unaffected by the inferred supersonic (Mach number $M \approx 3$) motion of this galaxy through the ICM of the Virgo cluster. This is because the galaxy and the high-$|z|$ gas lie behind a Mach cone with opening angle $\sim 80°$ (see Figure 7). The shocked ICM that flows near the galaxy has a velocity of $\sim$ 500 km s^{-1} and exerts insufficient ram pressure on the extraplanar gas to perturb its kinematics. In Veilleux et al. (1999b), we consider several explanations for the velocity field of the extraplanar gas. Velocities, especially blueshifted velocities on the N side of the galaxy, are best explained as a bipolar outflow which is tilted by $> 12°$ from the normal to the disk. The observed offset between the extraplanar gas and the radio structure may be due to buoyancy or refractive bending by density gradients in the halo gas.

5. SUMMARY AND FUTURE WORK

Over the past ten years, our group has obtained high-quality optical Fabry-Perot and long-slit spectrophotometry of a large sample of active galaxies. Many of these sources harbor wide-angle AGN-driven winds which can be of importance in the chemical and thermal evolution of the host galaxies. The high level of sophistication of recent hydrodynamical simulations (e.g., Suchkov et al. 1994; Strickland & Stevens 2000) has provided the theoretical basis to interpret our data and to predict the evolution and eventual resting place (disk, halo, or intergalactic medium) of the outflowing material. In the coming years, new ground-based observational techniques (e.g., tunable narrow-band filters, nod and shuffle techniques; Bland-Hawthorn 2000) and spacecrafts (e.g., Chandra and XMM) will allow us to put even stronger constraints on the influence of AGN-driven winds in nearby galaxies. These data will provide a critical local baseline for future surveys of high-redshift sources.

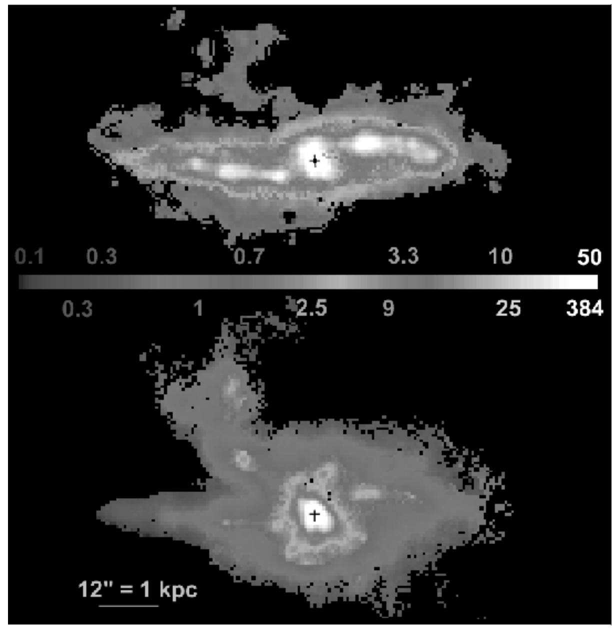

Fig. 6. The distributions of the line emission in NGC 4388. (top) Hα; (bottom) [O III] λ5007. North is at the top and East to the left. The spatial scale, indicated by a horizontal bar at the bottom of the image, corresponds to 12$''$, or 1 kpc for the adopted distance of 16.7 Mpc. The optical continuum nucleus is indicated in each panel by a cross.

S.V. is grateful for partial support of this research by a Cottrell Scholarship, NASA/LTSA grant NAG 56547, and NSF/CAREER grant AST-9874973.

REFERENCES

Balsara, D. S., & Krolik, J. H. 1993, ApJ, 402, 109
Begelman, M. C., McKee, C. F., & Shields, G. A. 1983, ApJ, 271, 70
Bicknell, G. V., Dopita, M. A., Tsvetanov, Z. I., & Sutherland, R. S. 1998, ApJ, 495, 680

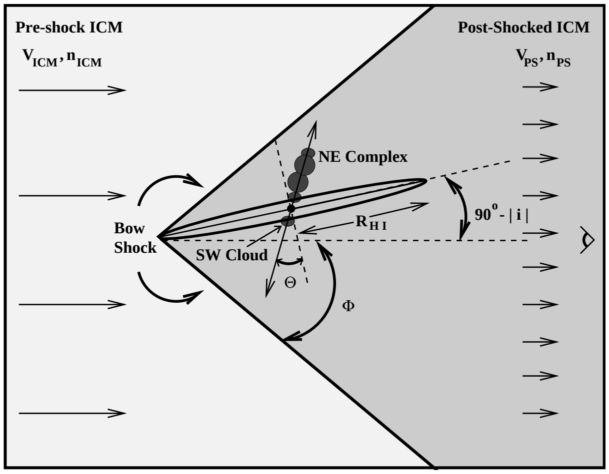

Fig. 7. Geometry of the interaction between NGC 4388 and the ICM. The values of the parameters indicated on this figure and discussed in Veilleux et al. (1999b) are: $i = -78°$, $\phi = 40°$, $\theta > 12°$, $R_{\rm H\,I} = 10$ kpc, $V_{\rm ICM} = 1500$ km s^{-1}, $n_{\rm ICM} \sim 10^{-4}$ cm^{-3}, $V_{\rm ps} = 500$ km s^{-1}, $n_{\rm ps} \sim 3 \times 10^{-3}$ cm^{-3}. The observer is located on the right in the same plane as the figure and at a distance of 16.7 Mpc.

Binette, L., Wilson, A. S., Storchi-Bergmann, T. 1996, A&A, 312, 365
Bland, J., & Tully, R. B. 1988, Nature, 334, 43
Bland-Hawthorn, J. 2000, Encyclopedia of Astronomy & Astrophysics
Bland-Hawthorn, J., Sokolowski, J., & Cecil, G. 1991, ApJ, 375, 78
Cayatte, V., Kotanyi, C., Balkowski, C., & van Gorkom, J. H. 1994, AJ, 107, 1003
Cecil, G. 1988, ApJ, 329, 38
Cecil, G., Bland, J., & Tully, R. B. 1990, ApJ, 355, 70
Cecil, G., Bland-Hawthorn, J., Veilleux, S., & Filippenko, A. V. 2001, ApJ, 555, 338
Cecil, G., et al. 2000, ApJ, 536, 675
Cecil, G., Ferruit, P., & Veilleux, S. 2002, RevMexAA(SC), 13, 170 (this volume)
Cecil, G., Morse, J., & Veilleux, S. 1995, ApJ, 445, 152
Cecil, G., Wilson, A. W., & Tully, R. B. 1992, ApJ, 390, 365
Cecil, G., Wilson, A. W., & de Pree, C. 1995, ApJ, 440, 181
Cecil, G., et al. 2002, ApJ, 568, 627
Colbert, E. J. M., Baum, S. A., Gallimore, J. F., O'Dea, C. P., & Christensen, J. A. 1996, ApJ, 467, 551
Colbert, E. J. M., Baum, S. A., O'Dea, C. P., & Veilleux, S. 1998, ApJ, 496, 786
Colina, L. 1992, ApJ, 386, 59
Corbin, M. R., Baldwin, J. A., & Wilson, A. S. 1988, ApJ, 334, 584
Dopita, M. A., & Sutherland, R. S. 1995, ApJ, 455, 468
Elmouttie, M., Haynes, R. F., Jones, K. L., Ehle, M., Beck, R., & Wielebinski, R. 1995, MNRAS, 275, L53
Elmouttie, M., Haynes, R. F., Jones, K. L., Sadler, E. M., & Ehle, M. 1998, MNRAS, 297, 1202
Falcke, H., Wilson, A. S., & Simpson, C. 1998, ApJ, 502, 199
Freeman, K. C., et al. 1977, A&A, 55, 445
Hummel, E., van Gorkom, J. H., & Kotanyi, C. G. 1983, ApJ, 267, L5
Krolik, J. H., & Begelman, M. C. 1986, ApJ, 308, L55
——————. 1988, ApJ, 329, 702
Marconi, A., Moorwood, A. F. M., Origlia, L., & Oliva, E. 1995, ESO Mess., 78, 20
Nagar, N. M., Vogel, S. N., Stone, J. M., & Ostriker, E. C. 1997, ApJ, 482, L195
Petitjean, P., & Durret, F. 1993, A&A, 277, 365
Phillips, M. M., & Malin, D. F. 1982, MNRAS, 199, 205
Pogge, R. W. 1988, ApJ, 332, 702
Shopbell, P. L., & Bland-Hawthorn, J. 1998, ApJ, 493, 129
Sokolowski, J., Bland-Hawthorn, J., & Cecil, G. 1991, ApJ, 375, 583
Stone, J. L., Wilson, A. S., & Ward, M. J. 1988, ApJ, 330, 105
Strikland, D. K., & Stevens, I. R. 2000, MNRAS, 314, 511
Suchkov, A. A., Balsara, D. S., Heckman, T. M., & Leitherer, C. 1994, ApJ 430, 511
Ulvestad, J. S., & Wilson, A. S. 1984, ApJ, 285, 439
Veilleux, S., & Bland-Hawthorn, J. 1997, ApJ, 479, L105
Veilleux, S., Bland-Hawthorn, J., & Cecil, G. 1999a, AJ, 118, 2108
Veilleux, S., Bland-Hawthorn, J., Cecil, G., Tully, R. B., & Miller, S. T.. 1999b, ApJ, 520, 111
Veilleux, S., Cecil, G., & Bland-Hawthorn, J. 1995, ApJ, 440, 181
Veilleux, S., Cecil, G., Bland-Hawthorn, J., Tully, R. B., Filippenko, A. V., & Sargent, W. L. W. 1994, ApJ, 433, 48
Veilleux, S., Shopbell, P. L., & Miller, S. T. 2001, AJ, 121, 198
Veilleux, S., Tully, R. B., & Bland-Hawthorn, J. 1993, AJ, 105, 1318
Ward, M., Penston, M. V., Blades, J. C., & Turtle, A. J. 1980, MNRAS, 193, 563

S. Veilleux: Dept. of Astronomy, University of Maryland, College Park, MD 20742 (veilleux@astro.umd.edu).
G. Cecil: Dept. of Physics and Astronomy, University of North Carolina, Chapel Hill, NC 27599-3255 (cecil@physics.unc.edu).
J. Bland-Hawthorn: Anglo-Australian Observatory, P.O. Box 296 Epping, NSW 2121 Australia (jbh@aaoepp2.aao.gov.au).
P. L. Shopbell: Dept. of Astronomy, California Institute of Technology, Pasadena, CA 91125 (pls@astro.caltech.edu).

Emission Lines from Jet Flows (Isla Mujeres, Q.R., México, November 13-17, 2000)
Editors: W. J. Henney, W. Steffen, A. C. Raga, & L. Binette